Examination of Fault-Ride-Through Methods for Off-Shore Wind Farms with VSC-Based Multi-terminal HVDC

U. Karaagac, J. Mahseredjian, H. Saad, S. Jensen, L. Cai

***Abstract*-- Fault ride-through (FRT) is a key aspect for offshore wind farms (OWFs) when connected to onshore ac grids through voltage source converter (VSC) based HVDC transmission system. The power flow from the OWFs cannot be reduced by the offshore VSCs during an onshore ac fault and the resulting power imbalance causes a fast increase in the dc network voltage. Without any special FRT method, the dc network voltage may increase up to intolerable levels and cause operation of dc overvoltage protection. This paper compares various FRT methods for a system of OWFs composed of doubly fed induction generator (DFIG) type wind turbines (WTs) and connected to an onshore ac grid through a multi-terminal (MT) modular multilevel converter (MMC) topology based VSC-HVDC. Various realistic onshore ac grid faults are simulated using EMTP-RV. The simulation results show that the implemented FRT methods limit the increase in dc network voltage and eliminate dc chopper requirement.**

***Keywords*: Fault-ride-through, offshore wind farm, doubly-fed induction generator, HVDC transmission, multi-terminal, voltage source converter, modular multilevel converter, EMTP.**

I. Introduction

THE planned offshore wind farms (OWFs) become larger and more distant from the onshore grid. The conventional HVAC transmission is not flexible and limited due to the large charging currents of cables. One alternative is to use point-to-point (PTP) HVDC systems for the connection of distant OWFs. Another approach is to interconnect several HVDC terminals to form a multi-terminal (MT) HVDC system. This approach offers several advantages, such as reduction in the number of HVDC converter terminals and possibility to transmit power in case of dc line outage. Therefore, MT-HVDC systems for OWFs are becoming more attractive.

The voltage source converter HVDC (VSC-HVDC) technology is based on insulated gate bipolar transistors (IGBTs) and it offers significant advantages over the thyristor-based line commutated converter HVDC (LCC-HVDC) technology, such as the ability to supply weak networks, black start capability and decoupled active and reactive power controls [1]. The overall footprints of converter stations are reduced as compared to LCC-HVDC. VSC-HVDC systems are more suitable for offshore applications [2].

Transmission System Operators (TSOs) stipulate a fault ride-through (FRT) capability of wind farms down to zero voltage for fault durations up to 150 ms [3], [4]. However, IGBT valves have no reverse blocking capability and the power flow from the OWFs cannot be interrupted by the offshore VSCs. As the onshore VSCs are not able to deliver the total OWF power to the onshore ac grid during faults, the resulting power imbalance charges the capacitances in the dc network. Without any countermeasures, the dc network voltage may increase up to intolerable levels and cause operation of the dc overvoltage protection of the HVDC system. This can be avoided by using a dc chopper (or choppers) to dissipate all the waste energy in breaking resistors. However, this solution leads to higher investment costs. Therefore, FRT methods based on fast reduction of power generation in OWFs have been discussed in recent literature [5]-[9]. These methods limit the dc network voltage increase and help reducing the size of the dc chopper or eliminate its requirement completely.

This paper illustrates the implementation of various FRT methods to a system of OWFs composed of doubly fed induction generator (DFIG) type wind turbines (WTs) and connected to an ac grid through a modular multilevel converter (MMC) topology based MT-HVDC. Various realistic onshore ac fault scenarios are simulated using EMTP-RV to compare the performances of the implemented FRT methods. The simulation results demonstrate that the implemented FRT methods limit the increase in dc voltage at tolerable values and eliminate the dc chopper requirement completely.

The first part of this paper presents the MMC-HVDC and DFIG systems briefly. The second part gives an overview on FRT methods and their implementation to an MT-HVDC connected OWF system. The simulated system and simulation results are presented in the last part.

II. Modular Multilevel Converter (MMC) HVDC

Recent trends on VSC-HVDC technology include MMCs.

U. Karaagac, J. Mahseredjian, H. Saad are with École Polytechnique de Montréal, Campus Université de Montréal, 2900, Édouard-Montpetit, Montréal (Québec), Canada, H3T 1J4.

S. Jensen, L. Cai are with Repower Systems AG, Überseering 10, D-22297, Germany.

Paper submitted to the International Conference on Power Systems Transients (IPST2013) in Vancouver, Canada July 18-20, 2013.

The MMC uses a stack of identical modules, each providing one step in the resulting multilevel ac waveform [10], [11]. Filter requirements are eliminated by using large number of levels per phase. Scalability to higher voltages is easily achieved and reliability is improved by increasing the number of SMs [12]. The MMC topology considered in this paper is based on the preliminary design of a 401-level MMC-HVDC system planned to interconnect the 400 kV networks of France and Spain by 2013 [13].

The onshore MMCs use a vector control strategy that calculates a voltage time area across the equivalent transformer/arm reactor which is required to change the current from present value to the reference value. The reference dq0-frame currents from the outer controller are calculated based on either pre-set AC and DC voltages, or pre-set active and reactive power. The inner controller permits controlling the converter AC voltage that will be used to generate the modulated switching pattern. The active and reactive currents in the dq0-frame can then be independently controlled via a proportional-integral (PI) control [14]. The reactive power control includes an AC voltage override block intended to maintain the voltage within acceptable limits.

The function of the offshore MMCs is to transmit the active power generated by the OWFs and to set a voltage reference for the DFIG type WT generators. As shown in Fig. 1, this is achieved using a simple voltage magnitude controller consisting of a PI regulator and feedback from measurement (v_{ac}). A fixed nominal frequency ($\hat{f}$) is supplied to the offshore MMC output voltage ($\hat{v}$). In other words, the offshore MMC is controlled as a voltage source with constant frequency and phase angle ($\hat{\theta}$). As the controller does not contain a current control, current limitation can be achieved by blocking IGBTs during a severe fault on the offshore ac network.

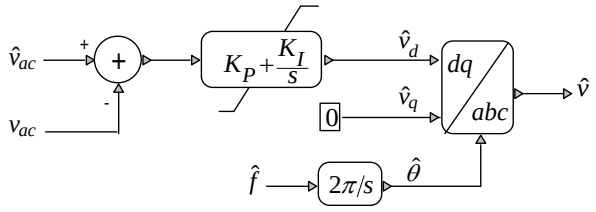

Fig. 1. Offshore MMC control.

III. DFIG Based Wind Turbines

The basic configuration of a DFIG WT is shown in Fig. 2. The stator of the wound rotor induction machine is connected directly to the power grid and the rotor is connected to the power grid through an ac-ac converter system. The ac-ac converter system consists of two three-phase pulse-width modulated (PWM) converters (grid-side and rotor-side converters) connected by a dc bus. A line inductor and an ac filter are used at the grid-side converter (GSC) to improve power quality. A crowbar is used to protect the rotor-side converter (RSC) against over-currents and the dc capacitors against over-voltages. During crowbar ignition, the RSC is blocked and the machine consumes reactive power. Therefore, the dc chopper is widely used to avoid crowbar ignition.

The control of the WT is achieved by controlling the RSC and GSC utilizing vector control techniques. Vector control allows decoupled control of both real and reactive power. The RSC controls the active and reactive powers delivered to the grid, and follows a tracking characteristic to adjust the generator speed for optimal power generation depending on wind speed. On the other hand, the GSC is used to maintain the dc bus voltage and to support the grid with reactive power during faults.

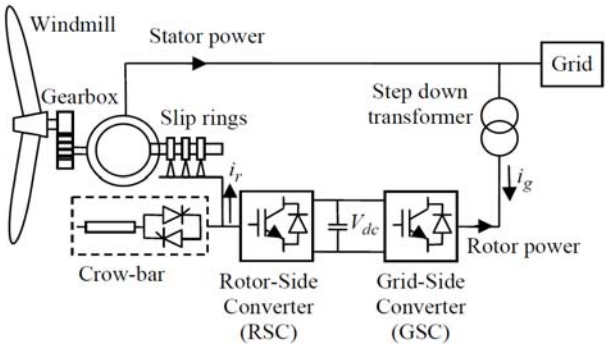

Fig. 2. Schematic diagram of a DFIG wind turbine.

IV. Fault Ride-Through (FRT) Methods

A. Active Current Reduction Through Offshore MMC

In this method, the offshore MMCs switch to decoupled power control mode following onshore ac fault detection and reduce the injected active power to the dc network. However, as the WTs are also operating in power control mode, the interaction between offshore MMCs and WT controls may lead to excessive overvoltages in the OWFs ac grid and mechanical stress on the WTs. Additional control algorithms can be implemented in WT controls to respond with power reduction to these overvoltages [5]. However, this method is less suitable in practice due to the slow rate of power reduction [8].

B. Active Current Reduction of WTs Through Power Reference Adjustment

In this method, the power reduction factor of the WTs is determined by a central dc voltage controller located at the offshore MMC (see Fig. 3). The dc voltage controller is activated when the dc network voltage exceeds a pre-specified limit and is deactivated again when it falls below the other pre-specified limit. It is a simple proportional control in which the power reduction factor (σ in Fig. 3) is calculated using the increase in dc network voltage in order to adjust the WT power output set value $\hat{P}$ as

$$\hat{P}' = (1+\sigma)\hat{P} \tag{1}$$

where $\hat{P}'$ is the adjusted WT electrical power output in pu.

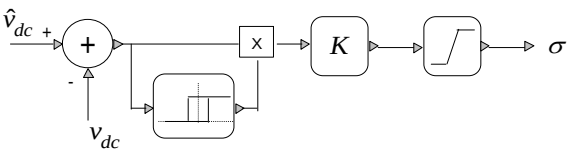

Fig. 3. Central dc voltage controller at offshore MMCs.

C. Active Current Reduction of WTs Through Frequency Control

This method eliminates the communication requirement between the central dc voltage controller and the WTs by increasing OWF frequency for power reduction. The central dc voltage controller in Fig. 3 is now used to adjust the frequency set value $\hat{f}$ of the offshore MMC control (see Fig. 1). However, it is difficult to measure fast frequency deviations in a fraction of a period [5] and this problem together with the slow response of the power controllers in the WTs are the limiting factors for the performance of this approach.

D. Voltage Reduction Through Offshore MMC Control

This method does not require communication between the central dc voltage controller and the WTs. It is based on fast voltage reduction in the OWF grid through offshore MMC voltage control and provides very fast reduction in OWF output power. It does not require any modifications in WT controls, but the voltage support through reactive current during voltage sags is recommended to be deactivated as it opposes to the fast voltage reduction in the OWF grid. On the other hand, implementing this method without deactivating the voltage support mechanism is not expected to cause a dramatic decline in its performance. The central dc voltage controller shown in Fig. 3 now used to adjust the voltage magnitude set value $\hat{v}_{ac}$ of the offshore MMC control (see Fig. 1) It should be noted that, sudden voltage reduction by the offshore MMC results in typical short-circuit currents with high dc components [15], high mechanical stress on the WT drive train, and electrical stress on the IGBTs of the MMC and DFIG converters. This may also cause a crowbar ignition, which also results into large mechanical stress and makes the generator system lose its controllability [16].

The performance of this method is improved in [7] and [8] with controlled demagnetization. High magnitude dc component currents resulting from sudden voltage drop at generator terminals are avoided by demagnetizing the machines in a fast and controlled way. The implementation of this method is improved further in [9] for the OWFs with PTP-HVDC connection. However, this method is well-suited for the OWFs with the PTP-HVDC connection. One implementation of this method is based on fault detection at the offshore MMC through dc voltage measurement, and controlled voltage drop based on additional dc voltage controller in the offshore MMC control [8]. The OWFs with MT-HVDC connection may contain more than one offshore MMC. Operating all offshore MMCs in dc voltage control mode may cause control interaction between offshore MMCs. The second implementation of this method is based on fault detection at the onshore MMC using ac voltage measurement, and controlled voltage drop based on communication between onshore and offshore MMCs. As the reduction factor of the offshore MMCs can be directly calculated from measured voltage sag at onshore MMCs, this implementation can be utilized for the OWFs with MT-HVDC connection. On the other hand, this measurement requires one complete cycle as it needs be done based on positive sequence onshore ac voltage due to unbalanced fault conditions. The other drawback of this implementation is the communication requirement between onshore and offshore MMCs which introduces a 10 to 20 ms additional time delay.

In this paper, the central dc voltage controller in Fig. 3 is used to eliminate the communication requirement between onshore and offshore MMCs. The dc offsets in the generator flux, i.e. high magnitude dc component currents resulting from sudden voltage drop at generator terminals, are avoided by an independent time-triggered voltage drop in all three phases in offshore MMC control, as shown in Fig. 4.

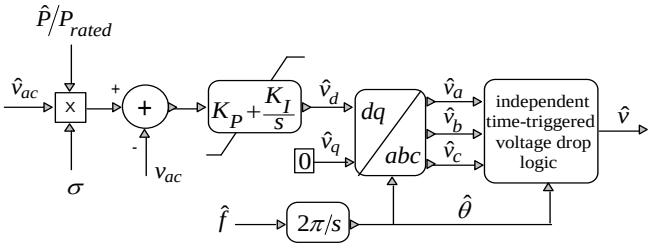

Fig. 4. Offshore MMC control with independent time-triggered voltage drop.

V. EMTP-RV Simulations

A. Simulated System

The EMTP-RV single line diagram of the simulated system is shown in Fig. 5. The MT-HVDC system is used to integrate up to 2 GW of offshore wind generation (from OWF-1 - OWF-10) through a transmission grid of single-core submarine cables modeled with frequency-dependent (wideband) models. The dc voltage is ±320 kV and the dc network is connected to the 400 kV, 50 Hz onshore ac grid at two different points. The GRID MMC-2 controls the power flow and onshore ac voltage, whereas the GRID MMC-1 controls dc network voltage and onshore ac terminal voltage.

Each of the 50 WTs, 200 MW OWF (OWF-1 - OWF-10 in Fig. 5) is divided into two clusters as shown in Fig. 6 and connected to offshore MMC through 150 kV single-core submarine cables modeled with coupled pi-section representation. Each cluster has five 34.5 kV radial feeders and each feeder contains the aggregated model of 2 MW, 60 Hz, DFIG type WTs. The equivalent parameters for the 34.5 kV equivalent feeders are calculated on basis of active and reactive power loss in the feeder for the rated current flow from each of the WTs [17].

MMCs and DFIG converters are represented with their average value models (AVMs). AVMs have been successfully developed for wind generation technologies [18], [19] and MMC-HVDC systems [20], [21]. In [22] and [23], it has been demonstrated that using AVM - AVM combination for MMCs and DFIG converters provides significant increase in simulation speed while maintaining sufficient accuracy.

The onshore ac system of Fig. 5 has been developed using a practical system presented in [24]. The 400 kV transmission network and loads in [24] have been modified by considering the additional 2 GW power injection from the OWFs. Each synchronous machine subnetwork (G in Fig. 5) contains a detailed machine model with controls (governor and exciter) and transformers. The loads are represented by equivalent impedances connected from bus to ground on each phase. The transmission lines are represented by distributed constant parameter models except the short lines between busses ALIAGA and ALIAGA HVDC. Coupled pi-section representation is used for those short lines. The 400 kV system is represented by an equivalent generator and load, to enable simulation of system behavior in case of a load or generating unit loss. The fault clearing times are 80 ms for local and 100 ms for remote circuit-breakers (CBs). The 110 ms breaker failure timer setting makes the fault clearing times 190 and 210 ms for local and remote backup CBs, respectively.

The initializations of MMC-HVDC and OWF models are achieved using voltage sources determined from a load-flow solution. The constant voltage sources are located at the network connection points of the MMCs. These sources provide fast initialization of the MT MMC-HVDC and OWFs, and also avoid transferring large initializing transient currents to the onshore ac grid. These sources are connected at the simulation startup and disconnected after 300 ms. The complete system reaches steady-state within 500 ms.

In the following simulations, the performance of the frequency control based FRT method (F-FRT) presented in IV.C, is compared with the voltage reduction based FRT method (V-FRT) presented in IV.D. The threshold dc voltage is set to 1.025 pu in both FRT methods. The central dc voltage controller gain (K in Fig. 3) is set to 10 (100% power reduction factor for 10% increase in dc voltage).

B. Simulated AC Fault Scenarios

Although several fault scenarios are simulated for different types of faults, only two of them are presented here due to space considerations. The first presented scenario (Scenario-1) is one of the practical scenarios that causes maximum voltage increase in dc network. In this scenario, a three-phase-to-ground fault is applied on ALIAGA HVDC end of one of 400-kV ALIAGA HVDC - ALIAGA lines at 0.75 s. The line circuit-breaker (CB) at ALIAGA substation is assumed to be stuck and the fault is cleared by the local backup CBs illustrated in Fig. 7, with open position following the operation of the busbar protection (at 0.96 s). The system is simulated for 3.5 s.

The second scenario (Scenario-2) is a 150 ms three-phase fault at the onshore GRID MMC-1 ac terminals (ALIAGA HVDC bus). This simulation is performed to test the system for the grid code requirement of Turkish Power System [4]. The fault is applied at 0.75 s and the system is simulated for 3.5 s.

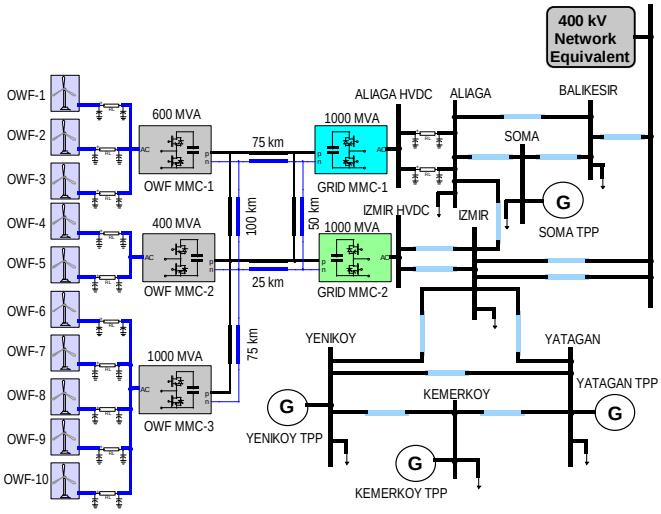

Fig. 5. EMTP-RV single line diagram of the simulated system.

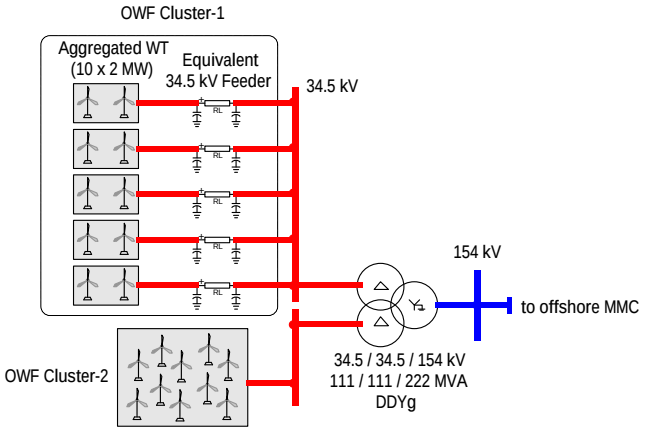

Fig. 6. EMTP-RV single line diagram of the 200 MW OWF.

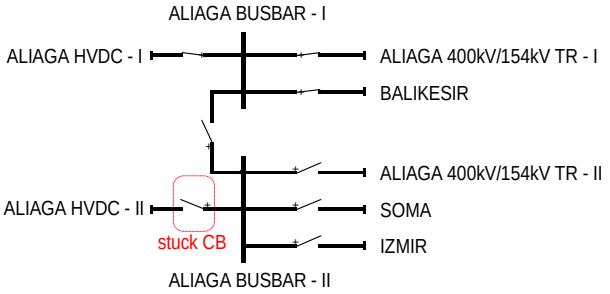

Fig. 7. Simplified single line diagram of ALIAGA substation.

C. Simulation Results

1) Scenario-1

The active power input to OWF MMC-1, the active power outputs of GRID MMC-1 and GRID MMC-2, and the dc

terminal voltage of GRID MMC-1 are presented in Fig. 8 - Fig. 11, respectively. It is seen in Fig. 8 that after fault detection through dc voltage measurement, both the F-FRT and V-FRT are initiated and limit the dc network voltage below 1.2 pu as shown Fig. 11. Hence both methods eliminate the dc chopper requirement without downgrading the safety or reliability of the system. It should be noted that, without any FRT method, the dc network voltage exceeds 1.3 pu even for the proper operation of the line circuit-breaker (CB) at ALIAGA substation. The dc overvoltage protection is normally triggered at 1.3 pu [5].

The performance of the F-FRT is better in this case compared to the PTP-HVDC case presented in [9]. This better performance is due to larger ratio of the dc network capacitance to the installed OWF capacity and the improved DFIG power controller for fast response. However, the response of F-FRT is still much slower compared to V-FRT. As a result, V-FRT limits the dc network voltage at a lower level compared to F-FRT.

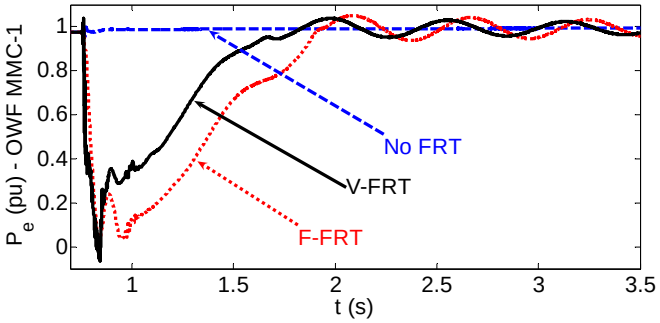

Fig. 8. Scenario-1, Active power input to OWF MMC-1.

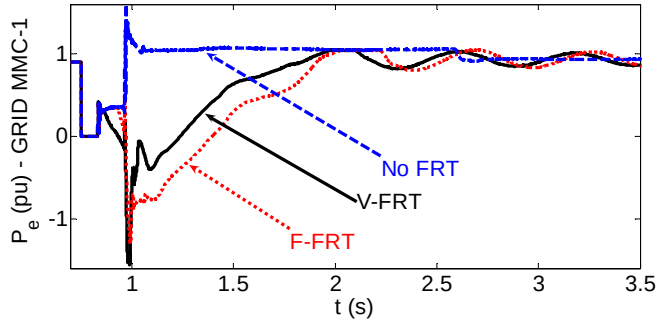

Fig. 9. Scenario-1, Active power output of GRID MMC-1.

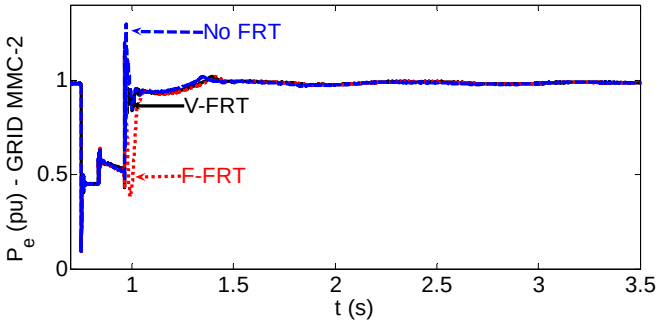

Fig. 10. Scenario-1, Active power output of GRID MMC-2.

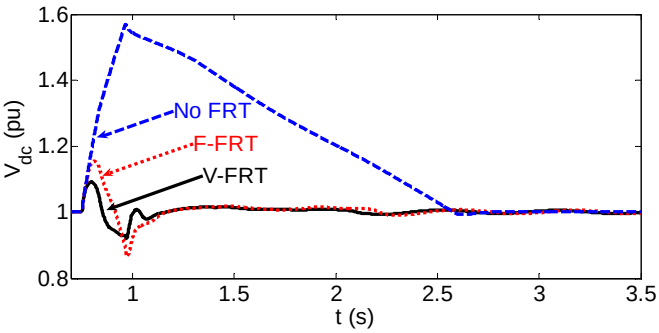

Fig. 11. Scenario-1, dc voltage at GRID MMC-1 terminal.

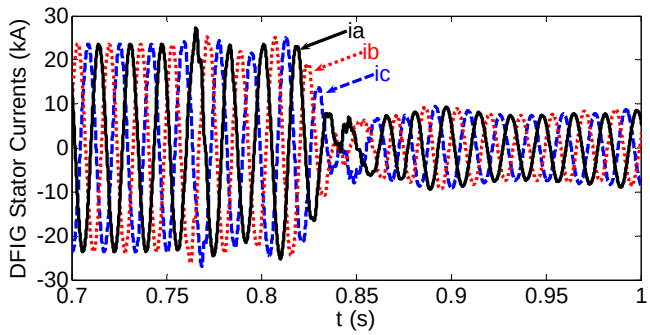

Fig. 12. Scenario-1, V-FRT, DFIG stator currents (10 DFIG aggregated unit at OWF-1, Cluster-1, Feeder-1).

The stator currents of the 10 DFIG aggregated unit representing the Feeder-1 of the Cluster-1 of the OWF-1 are presented in Fig. 12 for the V-FRT case. As seen from Fig. 12, independent time-triggered voltage drop in Fig. 4 prevents the high magnitude dc component currents resulting from sudden voltage drop at generator terminals.

1) Scenario-2

The active power input to OWF MMC-1 and the dc terminal voltage of GRID MMC-1 are given in Fig. 13 and Fig. 14, respectively. Both the F-FRT and V-FRT limit the dc network voltage below 1.2 pu as shown Fig. 14. Using either F-FRT or V-FRT, the grid code requirement can be satisfied without dc chopper usage and without downgrading the safety or reliability of the system.

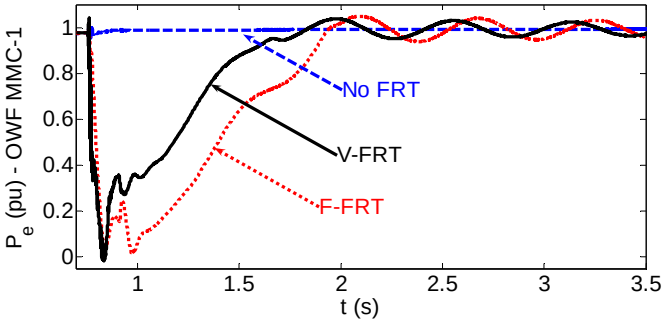

Fig. 13. Scenario-2, Active power input to OWF MMC-1.

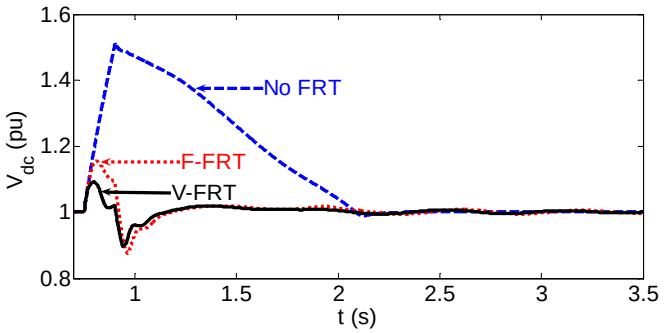

Fig. 14. Scenario-2, dc voltage at GRID MMC-1 terminal.

VI. Conclusions

This paper presented an overview on various FRT methods based on fast reduction of power generation in OWFs and discussed their implementations in OWFs with VSC based MT-HVDC. Two feasible methods, F-FRT and V-FRT, have been compared by simulating an OWF composed of DFIG type WTs and connected to a practical ac grid through a MMC based MT-HVDC. Even for the worst possible fault scenario, both methods limit the maximum dc overvoltage below 1.2 pu and eliminate the dc hopper requirement without downgrading the safety or reliability of the system. However, V-FRT provides faster power reduction and limits the dc network voltage at lower levels compared to F-FRT. The performance difference between V-FRT and F-FRT is expected to be more apparent for an OWF system having larger installed capacity ratio compared to the dc network capacitance.

VII. References

[1] N. Flourentzou, V. G. Agelidis, and G. D. Demetriades, "VSC-Based HVDC Power Transmission Systems: An Overview," *IEEE Trans. on Power Electronics*, vol. 24, no. 3, pp. 592-602, Mar. 2009.

[2] P. Bresesti, et al, "HVDC Connection of Offshore Wind Farms to the Transmission System," IEEE Transactions on Energy Conversion, vol. 22, no. 1, pp.37-43, March 2007.

[3] Hydro-Québec TransÉnergie, Transmission Provider Technical Requirements for the Connection of Power Plants to the Hydro Québec Transmission System, Feb. 2009.

[4] EMRA, "Wind Interconnection Rule Annex 18", Turkish Energy Market Regulatory Authority, Ankara, Nov. 2008.

[5] L. Harnefors, Y. Jiang-Häfner, M. Hyttinen, and T. Jonsson, "Ride-Through Methods for Wind Farms Connected to the Grid via a VSC-HVDC Transmission", http://www.abb.com.

[6] L. Xu, L. Yao, and C. Sasse, "Grid integration of large DFIG-based wind farms using VSC transmission", *IEEE Trans. Power Sys.*, vol. 22, no. 3, pp. 976-984, Aug. 2007.

[7] C. Feltes, H. Wrede, F. Koch, and I. Erlich, "Fault ride-through of DFIG-based wind farms connected to the grid through VSC-based HVDC link," in *Proc. 2008 PSCC 16th Power System Computation Conf.*

[8] C. Feltes, H. Wrede, F.W. Koch, and I. Erlich, "Enhanced fault ride-through method for wind farms connected to the grid through VSC-based HVDC transmission", *IEEE Trans. Power Sys.*, vol. 24, no. 3, pp. 1537-1546, Aug. 2009.

[9] U. Karaagac, H. Saad, J. Mahseredjian, S. Jensen and L. Cai, "Examination of Fault Ride-Through Methods for Off-Shore Wind Farms Connected to the Grid Through VSC-Based HVDC Transmission," in *11th International Workshop on Large-Scale Integration of Wind Power into Power Systems*, Lisbon, Portugal, Nov. 2012.

[10] A. Lesnicar and R. Marquardt, "An innovative modular multilevel converter topology suitable for a wide power range," in *Proc. IEEE Power Tech Conf.*, Bologna, Italy, Jun. 2003, vol. 3.

[11] G. Ding, G. Tang, Z. He, and M. Ding, "New Technologies of Voltage Source Converter (VSC) for HVDC Transmission System Based on VSC," *Proc. IEEE Power Eng. Soc. General Meeting*, pp. 1-8, Beijing, June 2008.

[12] B. Gemmell, J. Dorn, D. Retzmann, and D. Soerangr, "Prospects of Multilevel VSC Technologies for Power Transmission," in *Proc. IEEE Transmission and Distribution Conf. Exp.*, pp. 1-16, Milpitas, CA, Apr. 2008.

[13] J. Peralta, H. Saad, S. Dennetière, J. Mahseredjian and S. Nguefeu, "Detailed and Averaged Models for a 401-level MMC-HVDC system," *IEEE Transactions on Power Delivery*, vol.27, no.3, pp.1501-1508, July 2012.

[14] A. Lindberg, "PWM and Control of Two and Three level High Power Voltage Source Converters," Licentiate Thesis, Royal Institute of Technology, Stockholm, Sweden, 1995.

[15] M. S. Vicatos and J. A. Tegopoulos, "Transient state analysis of a doubly-fed induction generator under three phase short circuit," *IEEE Trans. Energy Convers.*, vol. 6, no. 1, pp. 62–68, Mar. 1991.

[16] I. Erlich *et al.*, "Modeling of wind turbines based on doubly-fed induction generators for power system stability studies," *IEEE Trans. Power Syst.*, vol. 22, no. 3, pp. 909–919, Aug. 2007.

[17] E. Muljadi, C.P. Butterfield, a Ellis, J. Mechenbier, J. Hochheimer, R. Young, N. Miller, R. Delmerico, R. Zavadil, and J.C. Smith, "Equivalencing the collector system of a large wind power plant," *2006 IEEE Power Engineering Society General Meeting*, 2006.

[18] J. Morren, S. W. H. de Haan, P. Bauer, J. Pierik, and J. Bozelie, "Comparison of complete and reduced models of a wind turbine with Doubly-fed Induction Generator," in *Proc. 10th Eur. Conf. Power Electron. Appl.*, Toulouse, France, Sep. 2003, pp. 1–10D.

[19] J. G. Slootweg, H. Polinder, and W. L. Kling, "Representing wind turbine electrical generating systems in fundamental frequency simulations," *IEEE Trans. on Energy Conversion*, vol. 18, no. 4, pp. 516-524, Dec. 2003.

[20] S. P. Teeuwsen, "Simplified dynamic model of a voltage-sourced converter with modular multilevel converter design," in *Proc. 2009 IEEE PES Power Syst. Conf. Expo.*, pp. 1-6.

[21] J. Peralta, H. Saad, S. Dennetière, J. Mahseredjian and S. Nguefeu, "Detailed and Averaged Models for a 401-level MMC-HVDC system," *IEEE Transactions on Power Delivery*, vol. 27, no. 3, pp. 1501-1508, July 2012.

[22] U. Karaagac, H. Saad, J. Mahseredjian, S. Jensen and L. Cai, "Off-Shore Wind Power Plant Modeling Precision and Efficiency in Electromagnetic Transient Simulation Programs," in *11th International Workshop on Large-Scale Integration of Wind Power into Power Systems*, Lisbon, Portugal, Nov. 2012.

[23] J. Peralta, H. Saad, U. Karaagac, J. Mahseredjian, S. Dennetière and X. Legrand, "Dynamic Modeling of MMC-based MTDC Systems for The Integration of Offshore Wind Generation," *CIGRE Canada conference on Power Systems*, September 2012, Montreal.

[24] U. Karaagac, J. Mahseredjian and O. Saad, "An efficient synchronous machine model for electromagnetic transients", IEEE Trans. on Power Delivery, vol. 26, no. 4, pp. 2456-2465, Oct. 2011.